H-mode edge physics in NSTX and Alcator C-Mod

F. Kelly
Unaffiliated
R. Maqueda
Nova Photonics
R. Maingi
Oak Ridge National Lab
and the NSTX Research Team
J. Hughes
MIT PSFC

49th APS-DPP Meeting
Nov. 12-16, 2006
Orlando, FL

Abstract

In NSTX (National Spherical Torus Experiment), ELMs (edge-localized modes) are observed using a fast-framing camera to interact with an inner-wall MARFE, leading to partial burn-through of the MARFE during the ELM cycle.[1] We reexamine the MARFE stability[2] to attempt an explanation of the MARFE/ELM dynamics in NSTX. The contribution of the ion self-diffusion to the radial electric field is estimated for an H-mode edge in Alcator C-Mod.

[1] R. Maqueda, et al., Bull. Am. Phys. Soc. **51** (7), 237 (2006); J. Nucl. Mater. **363-365**, 1000 (2007).
[2] F. Kelly et al., Bull. A Am. Phys. Soc. **51** (7), 237 (2006).
[3] A. Simon, Phys. Rev. **100**, 1557 (1955).
[4] C. L. Longmire and M. N. Rosenbluth, Phys. Rev., **103**, 507 (1956).

Introduction

- Large or Type I ELMs direct a substantial fraction of the plasma stored energy to the plasma-facing components (PFCs).
- The resulting erosion of PFCs over many pulses and the redistribution of the eroded material are critical issues that will affect the performance and operation of ITER or the proposed spherical torus (ST) concept for a Component Test Facility (CTF).
- The fast-evolving structure of MARFEs and ELMs is observed in NSTX using a Nova Photonics fast-framing camera.
- We apply basic thermal instability theory to assess interactions between MARFEs and ELMs in NSTX.
- The goal is a physics-based model and understanding to use in extrapolation for next generation ST and in ITER.
- The key physics for transport reduction is E × B velocity shear turbulence stabilization. Effects of E_r on transport enter only through derivatives of E_r. Can the ion self-collision flux help sustain a stationary H-mode or aid pedestal growth during an L-H transition?

MARFE evolution in high-density NSTX shot #117125

660.458 ms

‘average frame’ subtracted to enhance contrast

68000 frames/s or ~14.7 s between frames with a D_{α}-line bandpass filter

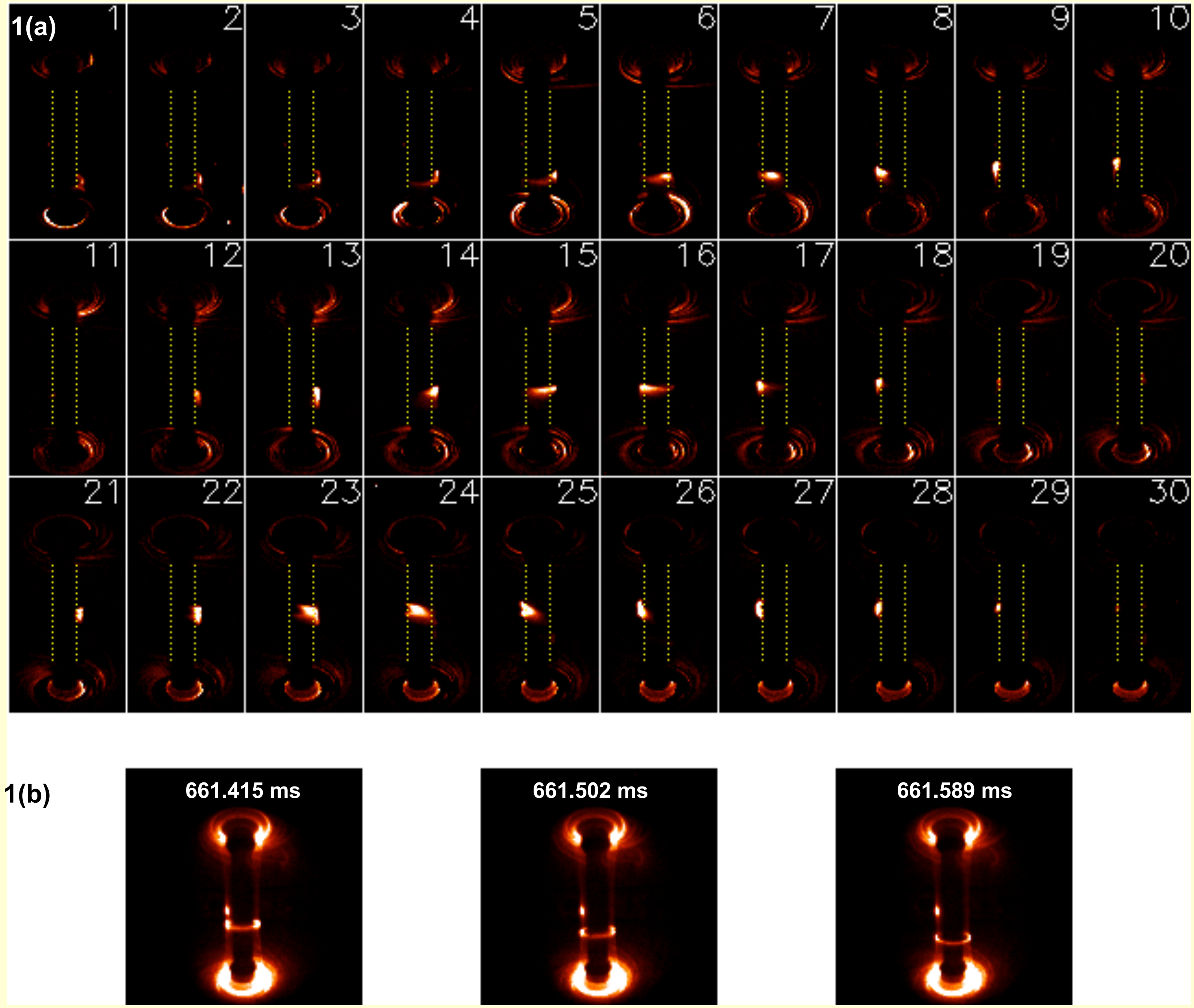

660.879 ms

MARFE/ELM dynamics observed in NSTX shot #117125 (900 kA, 6.2 MW, Double Null)

- Poloidally and toroidally localized MARFE remnant (plasmoid) moves upward following magnetic field line
- Plasmoid (MARFE precursor) upward movement stagnates and expands into a toroidally symmetric ring
- MARFE ring moves downward in ion ∇B drift direction
- ELM activity in divertor region coincides with burn through of most of MARFE

- Type I ELM (at ~665.5 ms) burns through MARFE

Downward drift in ion grad-B direction places stable MARFE position near lower divertor. Asakura, et al., NF 36, 795(1996)
Slight upper null bias places stagnation point near upper divertor.

ELM cycle drives dynamics of MARFE, remnant and precursor

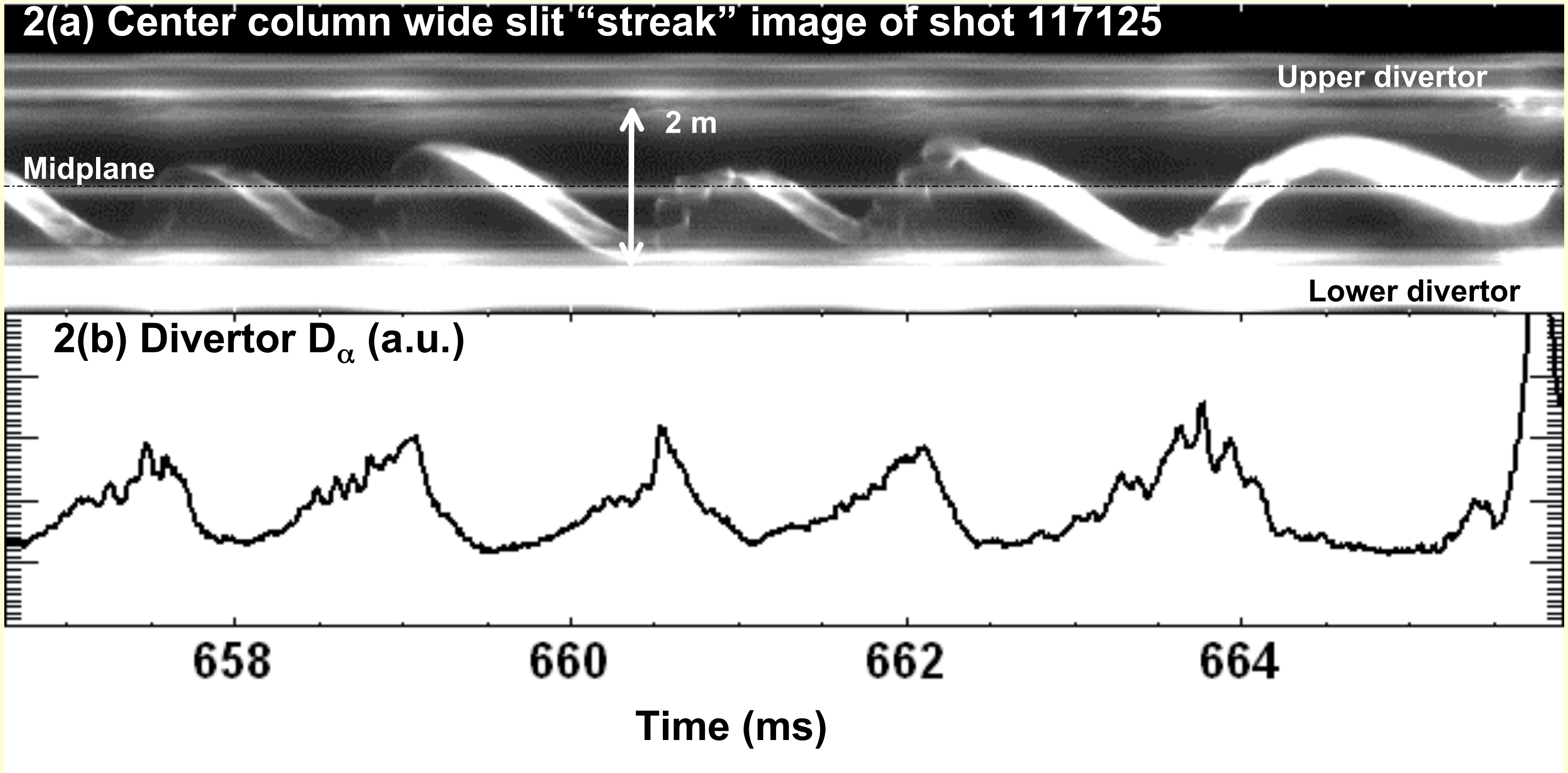

ELM cycle and MARFE cycle are closely linked, however, periods and lengths vary. Precursor of Type I ELM reverses MARFE movement and then burns through MARFE.

Basic MARFE theory

- Drake PF **30** (1987) found the MARFE to be a radiative condensation instability governed by the following linearized equation.

parallel and perpendicular conduction radiative condensation

$$\frac{5}{2}n\gamma\tilde{T} + k_{\parallel}^{2}\kappa_{\parallel}\tilde{T} - \kappa_{\perp}\frac{\partial^{2}\tilde{T}}{\partial r^{2}} = nn_{z}\left(\frac{2L_{z}}{T} - \frac{\partial L_{z}}{\partial T}\right)\tilde{T} \quad (1)$$

- Wesson and Hender NF **33** (1993) observed that the most unstable mode varies as cos θ and wave number $k_{\parallel} = 1/qR$

$$\kappa_{\perp}\frac{\partial^{2}\tilde{T}}{\partial r^{2}} - k_{\parallel}^{2}\kappa_{\parallel}\tilde{T} = nn_{z}T^{2}\frac{\partial}{\partial T}\left(\frac{L_{z}(T)}{T^{2}}\right)\tilde{T} \quad (2)$$

- Mahdavi, et al. 24^{th} EPS (1997) and Maingi and Mahdavi, FST **48** (2005), incorporated non-equilibrium radiation effect of neutrals in a uniform edge distribution, but neglected perpendicular conduction and atomic cooling to obtain an equation that is equivalent to

$$n_{marfe} \leq \sqrt{\frac{(\kappa_{0}/Z_{eff})T^{1/2}/(qR)^{2}}{-\sum_{z} f_{z}\frac{\partial}{\partial T}\left(\frac{L_{z}(T,f_{0})}{T^{2}}\right)}} \quad (3)$$

Mahdavi, et al. 24th EPS (1997) and Maingi and Mahdavi, FST **48** (2005), used an assumed a neutral fraction of $f_o = 0.001$ together with measured impurity concentrations of 1% carbon and 0.06% oxygen for two DIII-D shots: 89525 with $q_{95} = 9$ which marfed and 90323 with $q_{95} = 3.2$ which reached twice the Greenwald density without a MARFE. Defining the MARFE Index

$$MI \equiv \frac{n_{exp}}{n_{marfe}}$$

Eq. (3) results in $MI = 3.1 \times 10^{19}/2.94 \times 10^{19} = 1.05$ for shot 89525 and $MI = 3.4 \times 10^{19}/3.87 \times 10^{20} = 0.088$ for shot 90323. Stacey, Phys. Plasmas **9**, 2692 (2002) found shot 90323 at the MARFE threshold (MI = 1) by 2000ms, however the density continued to rise until a radiative collapse occurred at 2260 ms.

Application of Eq. (3) to the TEXTOR power scan series of shots analyzed in Kelly, Stacey, Rapp, and Brix, Phys. Plasmas **8**, 3382 (2001) resulted in a predicted MARFE density which exceeded the measured edge density by factor of ~3,as shown in the following slide. What is the relative importance of the parallel and perpendicular heat conduction different devices?

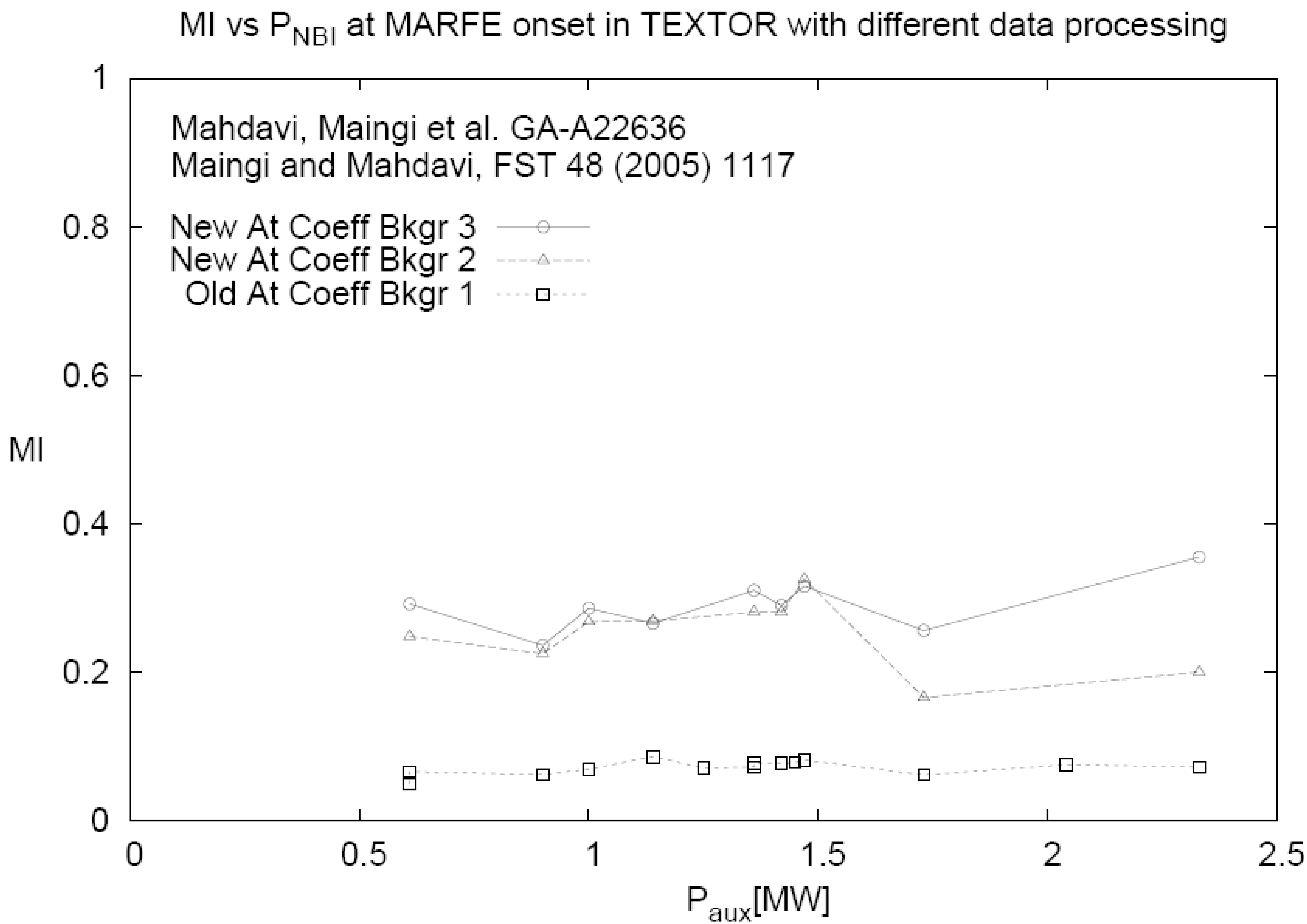
MI vs P_NBI at MARFE onset in TEXTOR with different data processing
Mahdavi, Maingi et al. GA-A22636
Maingi and Mahdavi, FST 48 (2005) 1117
New At Coeff Bkgr 3
New At Coeff Bkgr 2
Old At Coeff Bkgr 1
MI
P_aux[MW]
0
0.2
0.4
0.6
0.8
1
0.5
1.5
2
2.5

Table 1 MARFE stability observations for NSTX discharge 117125 at Thomson Scattering times, the MARFE Index at the preceding CHERS time and consistency with TEXTOR results (MARFE occurs if MI > 0.3) if $t_{TS} - t_{CHERS} < 1.5$ ms.

TS times (sec)	Condition	Preceding CHERS time	MI	Consistent
0.326662	no marfe	0.32525	0.101	yes
0.343345	no marfe	0.33525	0.086	
0.359992	no marfe	0.35525	0.201	
0.376685	upward move	0.37525	0.414	yes
0.393332	no marfe	0.38525	1.059	
0.410015	no marfe	0.40525	0.028	
0.426662	no marfe	0.42525	0.095	yes
0.443345	no marfe	0.43525	0.020	
0.459992	no marfe	0.45525	0.862	
0.476685	birth	0.47525	0.563	yes
0.493322	stagnation	0.48525	0.737	
0.510025	stagnation	0.50525	1.391	
0.526662	no marfe	0.52525	0.024	yes
0.543345	birth	0.53525	0.025	
0.559992	no marfe	0.55525	0.347	
0.576685	no marfe	0.57525	0.257	yes
0.593332	birth	0.58525	0.110	
0.610025	no marfe	0.60525	0.366	
0.626662	burn	0.62525	0.477	yes
0.643355	stagnation	0.63525	0.571	
0.660002	move down	0.65525	1.138	
0.676685	stable at top	0.67525	0.426	yes
0.693332	no marfe	0.68525	0.928	
0.710015	birth	0.70525	0.719	
0.726662	birth	0.72525	0.254	no
0.743355	no marfe	0.73525	0.146	
0.759992	no marfe	0.75525	0.075	
0.776685	no marfe	0.77525	0.099	yes
0.793332	no marfe	0.78525	0.074	
0.810015	stagnation	0.80525	0.269	

Cases: center image is nearest to TS time, left -72.5 μs, right +72.5 μs

0 = no marfe; t = 0.326662 s

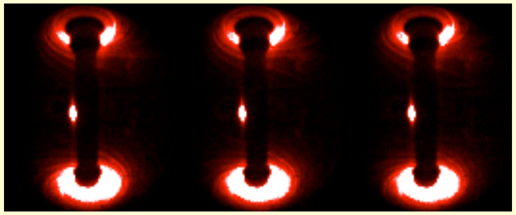

3 = stagnation; 0.493322 s

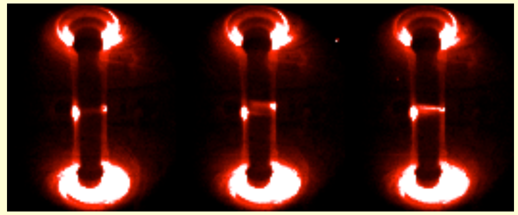

6 = stable at top; 0.676685 s

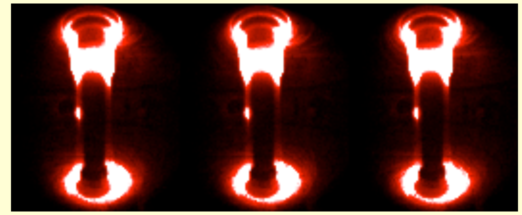

1 = marfe birth; 0.726662 s

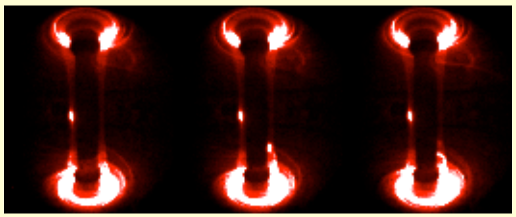

4 = move down; 0.660002 s

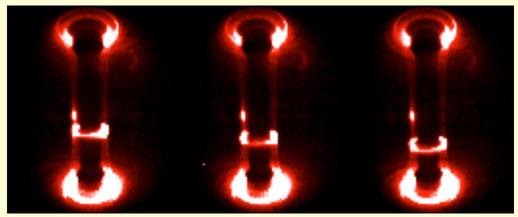

NSTX discharge
117125

2 = move up; 0.376685 s

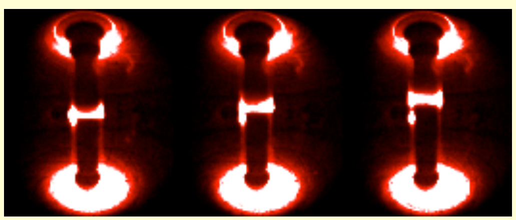

5 = burn; 0.626662 s

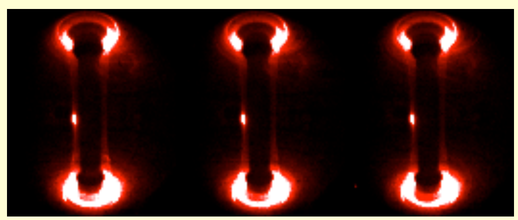

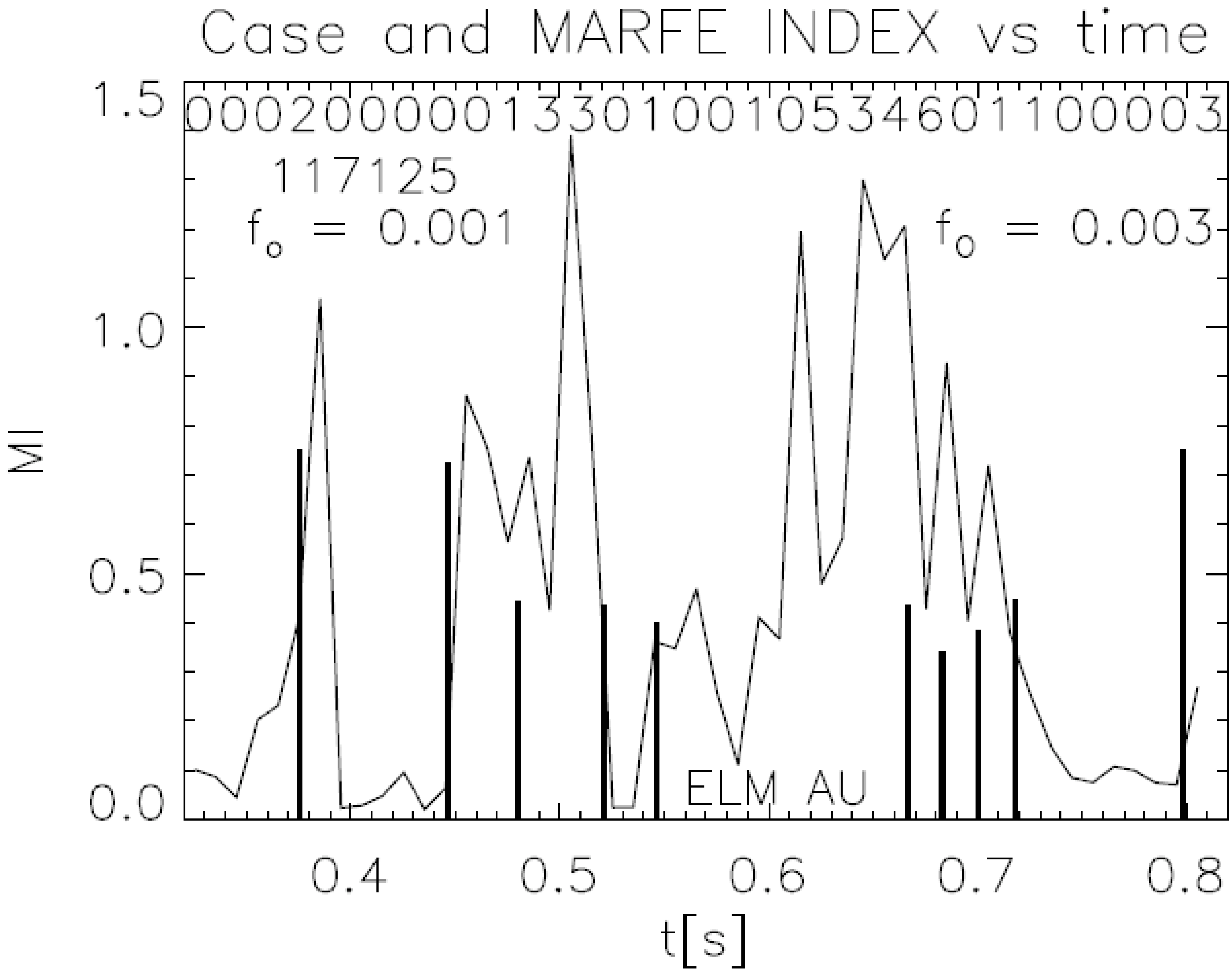
Case and MARFE INDEX vs time
000200000133010010534601100003
117125
f_o = 0.001
f_o = 0.003
ELM AU
MI
t[s]
1.5
1.0
0.5
0.0
0.4
0.5
0.6
0.7
0.8

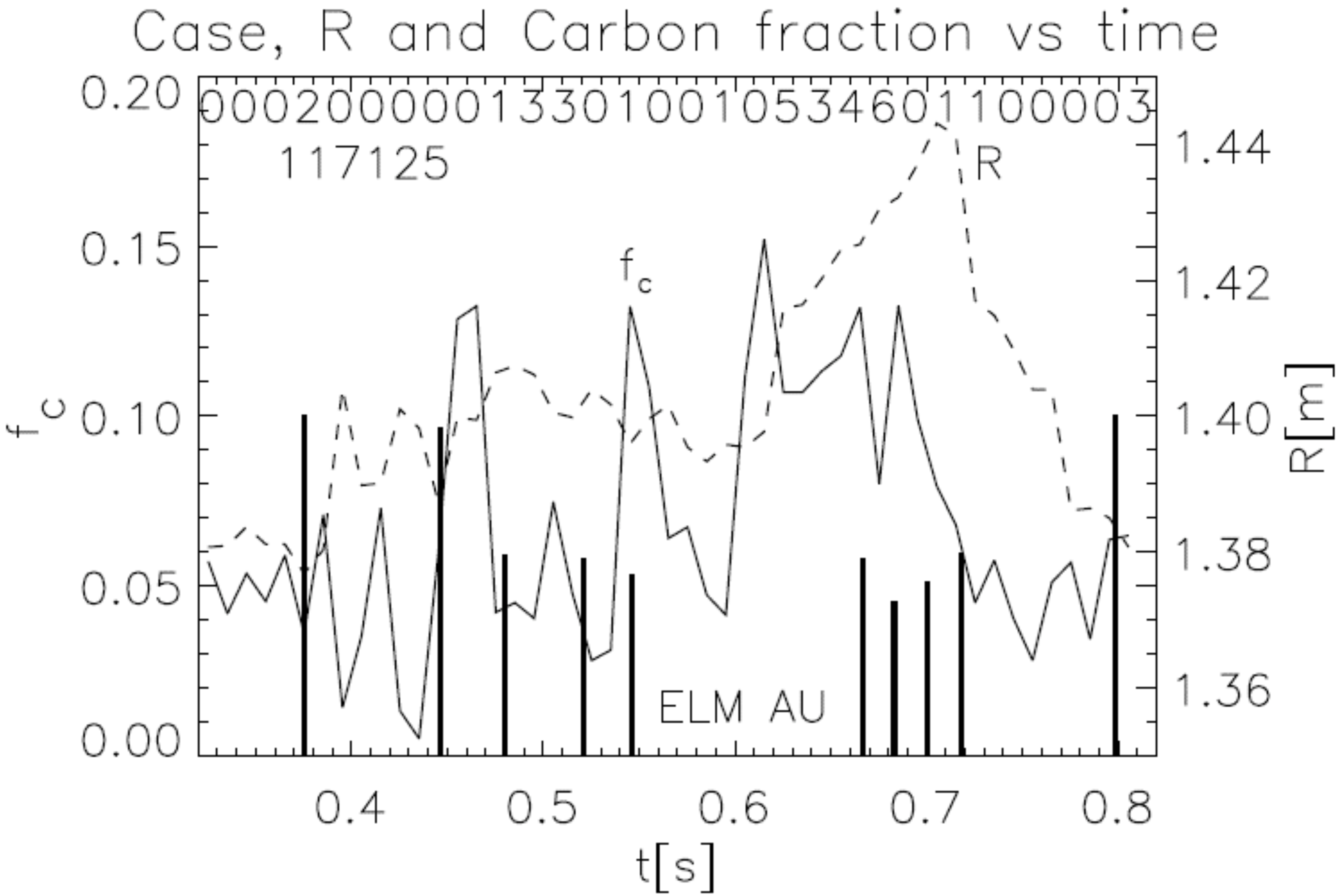
Case, R and Carbon fraction vs time
000200000133010010534601100003
117125
R
f_c
ELM AU
0.20
0.15
0.10
0.05
0.00
1.44
1.42
1.40
1.38
1.36
0.4
0.5
0.6
0.7
0.8
t[s]
f_c
R[m]

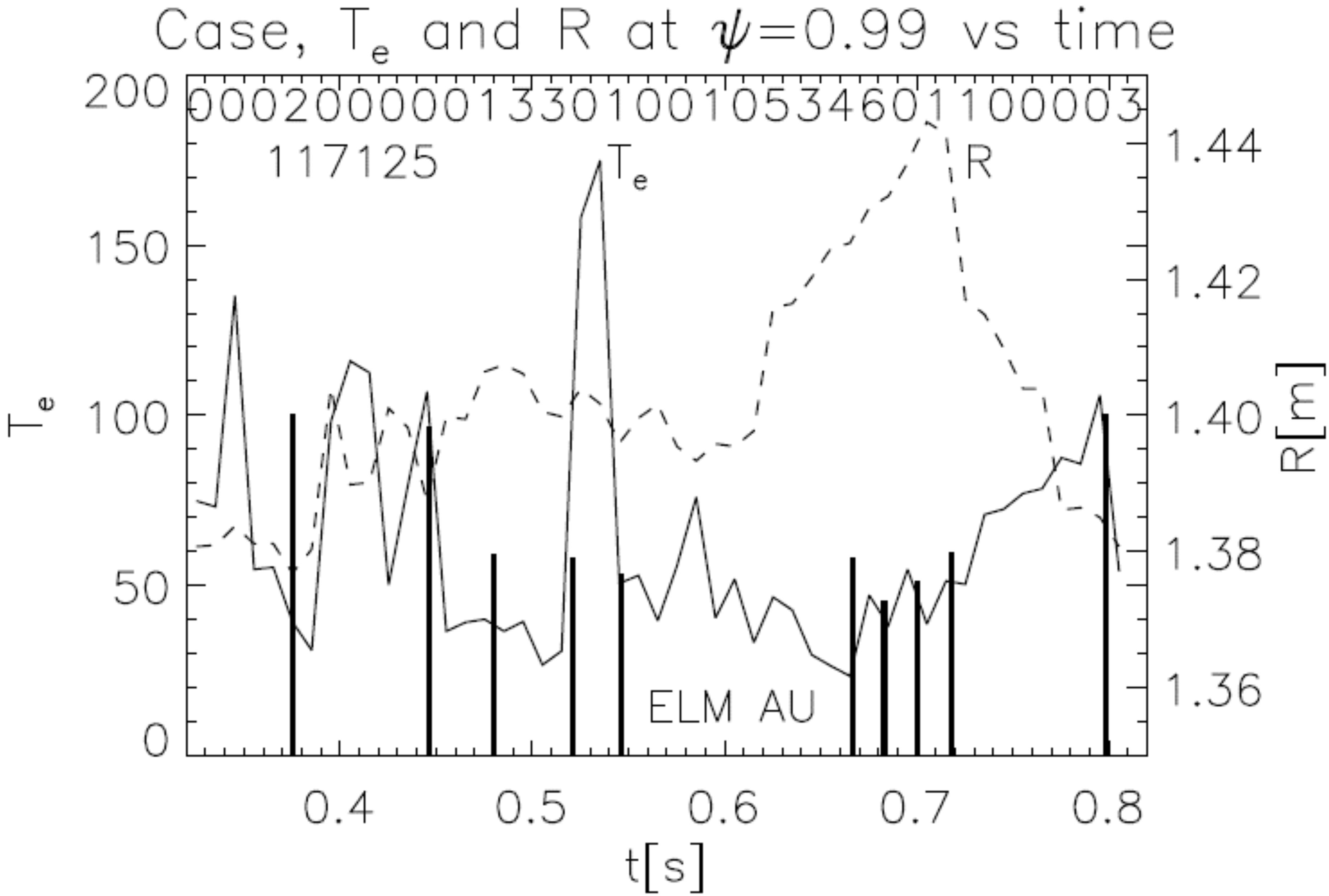
Case, T_e and R at ψ=0.99 vs time
000200000133010010534601100003
117125
T_e
R
ELM AU
T_e
R[m]
t[s]
0
50
100
150
200
1.36
1.38
1.40
1.42
1.44
0.4
0.5
0.6
0.7
0.8

MARFE Movement – ExB Drift and Experimental Estimates

- Shot 110077 of NSTX: DN, D fueled, $B_T(0)$ = -0.45 T, I_p = 1 MA and P_{NBI} up to 5.1 MW during an H-mode edge during which the LFS radial electric field has been estimated[2] to be between 0 and -5 kV/m.

- If for NSTX shot 117125, with similar conditions, we assume a similar variation of E_r on the high field side. $V_E=E_r/B$ varies between 0 and -3 km/s downward in the ion grad-B drift direction.

- From Fig. 1(b), the ring MARFE at 661 ms moves about 0.20 m downward in 0.174 ms for an experimental poloidal velocity of -1.1 km/s. Similarly, we estimate that the ring MARFE at 377 ms moves upward 0.20 m in 0.145 ms, 1.6 km/s.

[2] T. M. Biewer, et al., Rev. Sci. Instr. **75**, 650 (2004).

MARFE Movement – Diamagnetic Drift

- Heat balance eq. with conductive diamagnetic heat flux and terms describing the dependencies of the pressure, P, on time, t, and poloidal angle, θ, and assuming the other terms constant[3], we may write

$$\frac{3}{2}\frac{\partial P}{\partial t} + \frac{5}{2}(1 - \alpha_T \alpha_P)\frac{q_b}{eB\kappa_\perp a}\frac{\partial P}{\partial \theta} = C$$

$q_b = \bar{q}_b(1 - \beta\cos\theta)$ the power loss through the plasma core-edge boundary

$\bar{q}_b = Q_b / A_p$ Q_b is the net power transported through area A_p

$\alpha_T \equiv \nabla_r T_i / \nabla_r T_e$ and $\alpha_P \equiv P_i / P_e$

- Taking perturbations of P of the form $\tilde{P} \propto \exp(V_{\vartheta d} t - a\theta)$ we estimate the poloidal diamagnetic drift velocity to be $V_{\theta d} = \frac{5}{3}\frac{q_b}{eB\kappa_\perp}(1 - \alpha_T \alpha_P)$
- Using Thomson measurements of n_e and T_e and CHERS measurements of n_i and T_i on the LFS we estimate for shot 117125

  $\alpha_T = 1.0$ and $\alpha_P = 1.8$ at 661 ms => $V_{\theta d} \sim 0.8$ km/s upward

  $\alpha_T = 0.5$ and $\alpha_P = 7.4$ at 377 ms => $V_{\theta d} \sim 3.3$ km/s upward
- If total drift velocity due to the sum of the ExB and diamagnetic drifts, implies ExB drift is 2.4 km/s downward (HFS E_r = -1.4 kV/m) at 661 ms and 2.2 km/s downward (HFS E_r = -1.1 kV/m) at 377 ms

[3] M. Z. Tokar, Contrib. Plasma Phys. **32**, 341 (1992).

Ion self-collision driven flux

- It is well known that the lowest-order diffusive flux from like-particle collisions vanishes and that to obtain a non-zero net flux one must retain higher order terms[4] as in the classical theory of Simon[5] and Longmire and Rosenbluth[6] .

$$\Gamma_{ii}^{cl} = \frac{8}{15\pi}\left(\frac{kT_i}{m_i}\right)^2 \frac{n_i}{\tau_{ii}\,\Omega_i^{\,4}} \frac{d}{dr}\left(\frac{1}{n_i}\frac{d^2 n_i}{dr^2}\right)$$

- This flux is small compared to that arising from unlike-particle collisions when the variation in density is small over a Larmor radius. However, may be significant in the H-mode steep density gradient region.

- A more rigorous analysis would include the neo-classical contribution[7-9] of the diffusive flux to the radial electric field. However, the analysis outside the core, including neutral particles, is difficult and has not been done[10].

[4] R. J. Goldston and P. H. Rutherford, Introduction to Plasma Physics, IOP Publishing Ltd, 1995.
[5] A. Simon, Phys. Rev. **100**, 1557, (1955).
[6] C. L. Longmire and M. N. Rosenbluth, Phys. Rev. **103**, 507 (1956).
[7] W. X. Wang, W. M. Tang and W. W. Lee, Phys. Rev. Lett. **78**, 456 (1997).
[8] W. X. Wang, F. L. Hinton and S. K. Wong, Phys. Rev. Lett. **87**, 055002 (2001).
[9] W. X. Wang, W. M. Tang, F. L. Hinton, et al., Comp. Phys. Comm. **164**, 178 (2004).
[10] W. X. Wang, personal communication, 2007.

Classical radial electric field due to ion self-collision driven flux

Ambipolar radial electric field

$$E_r^{cl} = \frac{\Gamma_{ii}^{cl}}{n\left(\mu_e - \mu_i\right)}$$

$$where\ \mu_e = -\frac{m_e \nu_e}{e B^2}\ and\ \mu_i = \frac{m_i \nu_i}{e B^2}\ for\ cylindical\ geometry\ \left(slide\ 19\right)$$

$$\mu_e = -\frac{m_e \nu_e}{e {B_\theta}^2}\ and\ \mu_i = \frac{m_i \nu_i}{e {B_\theta}^2}\ toroidal\ geometry\ with\ \mathrm{v}_{i\theta} = 0\ \left(slide\ 20\right)$$

Average ion and electron momentum loss rates due to collisions

$$\nu_e = \nu_{ee} + \nu_{ei} + \nu_{en},\ where\ \nu_{en} = \sigma_{neut}\, n_n\, \mathrm{v}_{th,e}\ and\ \sigma_{neut} = 3\times 10^{-20}\ m^2$$

$$\nu_i = \nu_{ie} + \nu_{ii} + \nu_{in},\ where\ \nu_{in} = n_n \left(\left\langle \sigma\, \mathrm{v}\right\rangle_{cx} + \left\langle \sigma\, \mathrm{v}\right\rangle_{el}\right)$$

Experimental estimate of E_r in Alcator C-Mod H-mode edge by W. L. Rowan

E_r = -1 kV/m

Density profiles

Assumed tanh density profile

$$n(R) = b + \frac{h}{2}\left[\tanh\left(\frac{R_0 - R}{d}\right) + 1\right] + m\left(R_0 - R - d\right)H\left(R_0 - R - d\right)$$

$$H(x) = \begin{cases} 0, & x < 0 \\ 1, & x \geq 0 \end{cases}$$

Ion self-collision flux

$$\Gamma_{ii}^{cl} = \frac{8}{15\pi}\left(\frac{kT_i}{m_i}\right)^2 \frac{1}{\tau_{ii}\,\Omega_i^{\,4}} \times$$

$$\frac{\left(\frac{dy}{dR}\right)^3 \left\{-h\left[1 - 4\tanh^2 y + 3\tanh^4 y\right]\left[b + \frac{h}{2}\left(\tanh y + 1\right)\right] + \frac{h^2}{2}\tanh y\left[1 - \tanh^2 y\right]^2\right\}}{b + \frac{h}{2}\left(\tanh y + 1\right)}$$

$$\textit{where } y = \frac{R_0 - R}{d}$$

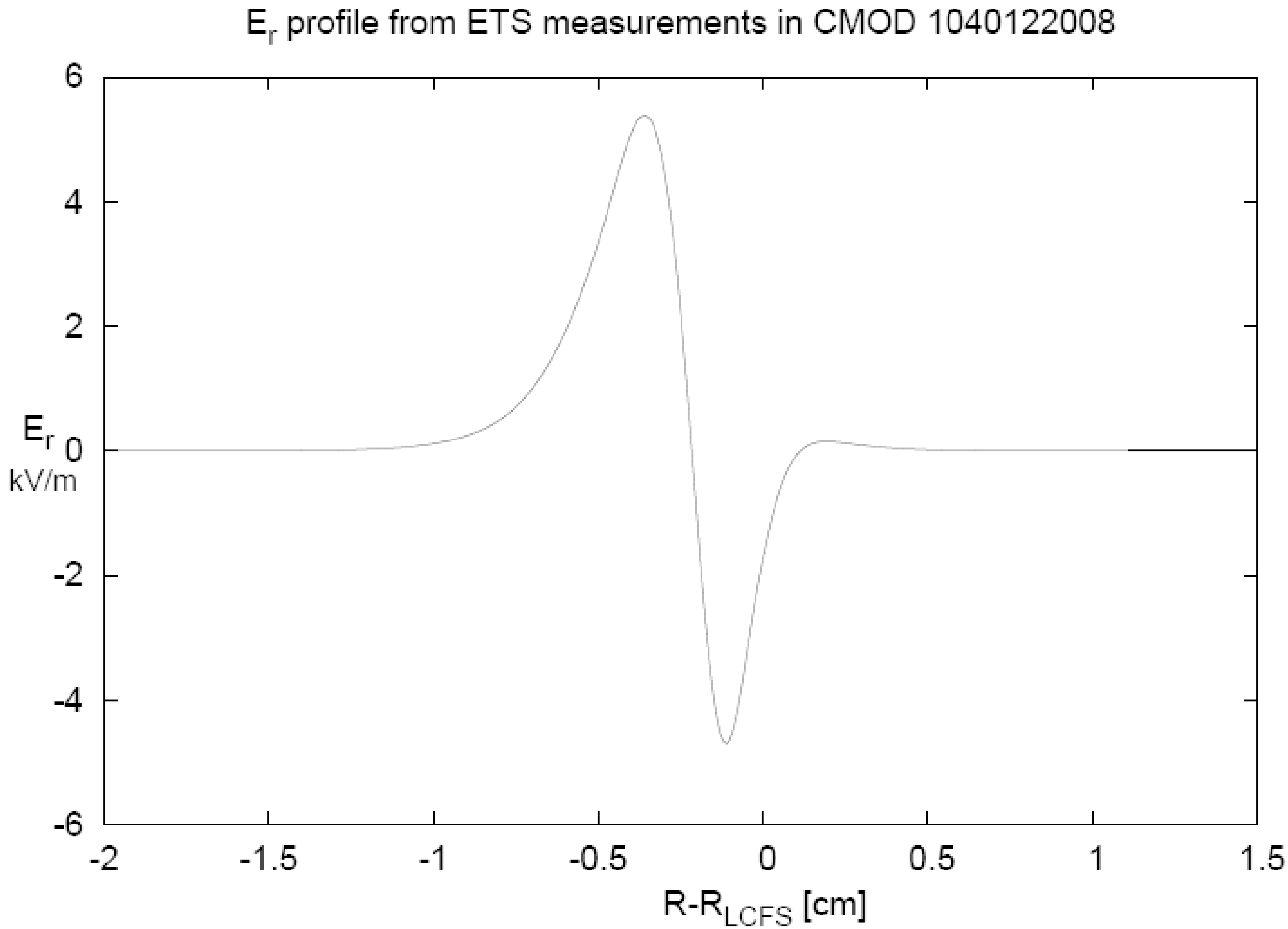
E_r profile from ETS measurements in CMOD 1040122008
E_r
kV/m
6
4
2
0
-2
-4
-6
-2
-1.5
-1
-0.5
0
0.5
1
1.5
R-R_LCFS [cm]

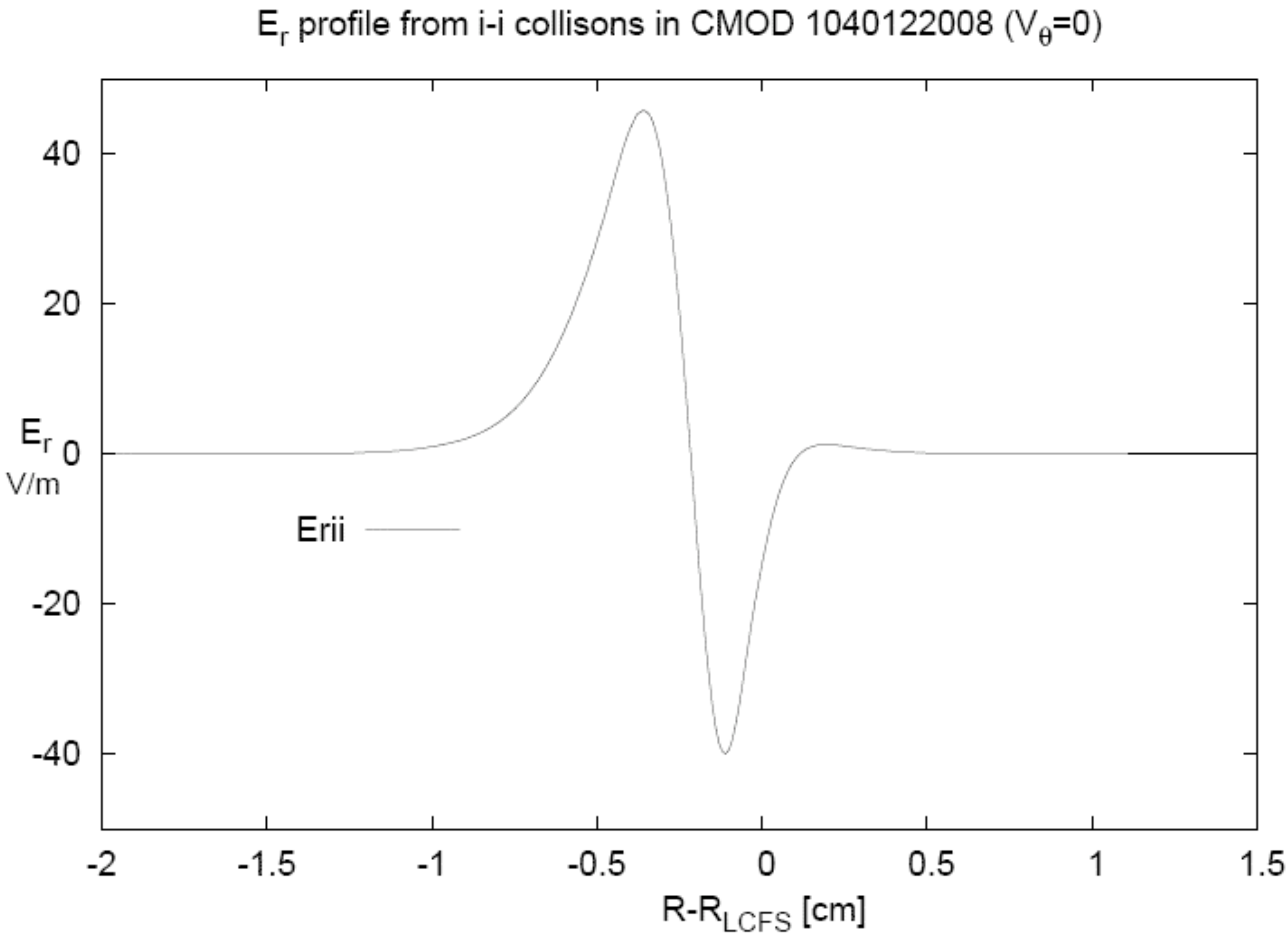
E_r profile from i-i collisons in CMOD 1040122008 (V_θ=0)
40
20
0
-20
-40
E_r
V/m
Erii
-2
-1.5
-1
-0.5
0
0.5
1
1.5
R-R_LCFS [cm]

Discussion of Results

- ELMs releases pulse of heat and particles inside the separatrix affecting MARFE condition and movement by increasing the LFS edge temperature and parallel pressure gradient and initially reducing the edge carbon density. Large ELMs erode carbon from the divertor and increase carbon density.
- Movement of the LFS separatrix outward tends to increase edge carbon fraction and MARFEs, while inward movement tends to decrease edge carbon fraction and large ELMs.
- MARFEs and ELMs have a time scale of less than 1 ms. CHERs measurements of carbon are averaged over ~10 ms and Thomson scattering measurements occur at 60 Hz with coarse spatial resolution, it is not currently possible to resolve the MARFE condition from experimental data.
- Theory indicates the general tendency for MARFEs to form. However, theory strictly applies to conditions before MARFE formation, not during MARFE. Table 1 shows that the MARFE theory of Mahdavi and Maingi is consistent (9 of 10) with experimental data from NSTX compared with results from TEXTOR.
- Uncertainty in the separatrix location and the temporal and spatial resolution of the plasma diagnostics limit the comparison.
- The movement of MARFEs in NSTX is consistent with the sum of diamagnetic and ExB drift, if the HFS E_r is about -1 kV/m.
- Component of E_r in Alcator C-MOD due to ion self-diffusion bounds the experimentally estimated E_r , but depends of the unknown $V_{i\theta}$. If $V_{i\theta} \approx 0$, then the contribution of ion self-diffusion to E_r is negligible.

Conclusions

• The basic MARFE theory of Mahdavi and Maingi, which includes only parallel heat conduction, predicted the MARFE state in two DIII-D shots but consistently over predicted the density limit, nMARFE, in a power scan series of TEXTOR shots. If the TEXTOR results are considered to be more indicative, MARFE onset in NSTX is found to be consistent with the TEXTOR results in 9 out of 10 Thomson Scattering (TS) times where CHERS data is available less than 1.5 ms before. This CHERS data is integrated over a period that is centered on the TS times and should yield the best comparison.

• The NSTX plasma edge is a very dynamic region with ELMs initially removing carbon impurity from the plasma edge, but large ELMs eroding carbon from the divertor increasing the amount of carbon in the plasma. The movement of the inner and outer separatrix in NSTX shot 117125 complicates the analysis. The inner separatrix was considered to be better determined and used to shift the LFS profiles to align with the HFS profiles. Large excursions in T_e and n_e at the 99% flux surface suggest the inner separatrix is sometimes not well determined. Improved location of the separatrix and better spatial and temporal resolution of the diagnostics are needed to facilitate comparison of the theory with experiment.

• The contribution of ion self-collision to the radial electric field requires rotation data to be resolved.